frontiers | Frontiers in Materials

TYPE Original Research
PUBLISHED 12 January 2023
DOI 10.3389/fmats.2023.1022878

OPEN ACCESS

EDITED BY
Kulwinder Kaur,
Mehr Chand Mahajan DAV College for Women Chandigarh, India

REVIEWED BY
Way Foong Lim,
University of Science Malaysia (USM), Malaysia
Rabia Yasmin Khosa,
University of Education Lahore, Pakistan

*CORRESPONDENCE
Xiaodong Pi,
✉ xdpi@zju.edu.cn
Rong Wang,
✉ rong_wang@zju.edu.cn

SPECIALTY SECTION
This article was submitted to Semiconducting Materials and Devices, a section of the journal Frontiers in Materials

RECEIVED 19 August 2022
ACCEPTED 02 January 2023
PUBLISHED 12 January 2023

CITATION
Gao W, Yang G, Qian Y, Han X, Cui C, Pi X, Yang D and Wang R (2023), Dislocation-related leakage-current paths of 4H silicon carbide.
Front. Mater. 10:1022878.
doi: 10.3389/fmats.2023.1022878

Dislocation-related leakage-current paths of 4H silicon carbide

Wandong Gao[1,2], Guang Yang[3], Yixiao Qian[1,2], Xuefeng Han[1,2], Can Cui[3], Xiaodong Pi[1,2]*, Deren Yang[1,2] and Rong Wang[1,2]*

[1]State Key Laboratory of Silicon and Advanced Semiconductor Materials and School of Materials Science and Engineering, Zhejiang University, Hangzhou, Zhejiang, China, [2]Institute of Advanced Semiconductors and Zhejiang Provincial Key Laboratory of Power Semiconductor Materials and Devices, ZJU-Hangzhou Global Scientific and Technological Innovation Center, Hangzhou, Zhejiang, China, [3]Key Laboratory of Optical Field Manipulation of Zhejiang Province, Department of Physics, Zhejiang Sci-Tech University, Hangzhou, Zhejiang, China

Improving the quality of 4H silicon carbide (4H-SiC) epitaxial layers to reduce the leakage current of 4H-SiC based high-power devices is a long-standing issue in the development of 4H-SiC homoepitaxy. In this work, we compare the effect of different type of dislocations, and discriminate the effect of dislocation lines and dislocation-related pits on the leakage current of 4H-SiC by combining molten-KOH etching and the tunneling atomic force microscopy (TUNA) measurements. It is found that both the dislocation lines of threading dislocations (TDs) and the TD-related pits increase the reverse leakage current of 4H-SiC. The dislocation lines of TDs exert more significant effect on the reverse leakage current of 4H-SiC, which gives rise to the nonuniform distribution of reverse leakage current throughout the TD-related pits. Due to the different Burgers vectors of TDs, the effect of TDs on the reverse leakage current of 4H-SiC increases in the order to threading edge dislocation (TED), threading screw dislocation (TSD) and threading mixed dislocation (TMD). Basal plane dislocations (BPDs) are also found to slightly increase the reverse leakage current, with the leakage current mainly concentrated at the core of the BPD. Compared to the effect of TDs, the effect of BPDs on the reverse leakage current of 4H-SiC is negligible. Our work indicates that reducing the density of TDs, especially TMDs and TSDs, is key to improve the quality of 4H-SiC epitaxial layers and reduce the reverse leakage current of 4H-SiC based high -power devices.

KEYWORDS

4H silicon carbide, epitaxial layers, tunneling atomic force microscopy, dislocations, leakage current

1 Introduction

The superior properties of 4H silicon carbide (4H-SiC) such as wide bandgap, high breakdown electric field strength, and high thermal conductivity, have endowed 4H-SiC based high-power electronics great success in industrial motor drives, electric transportations and new-energy converters (Cooper and Agarwal, 2002; Kimoto and Cooper, 2014; Wang et al., 2020). Compared with other wide-bandgap semiconductors, owing to the great success of the single-crystal growth and wafer processing of 4H-SiC substrates, the homoepitaxy of 4H-SiC has the advantages of low dislocation density and high reliability, which facilitate the industrialization of 4H-SiC based high-power devices. Furthermore, the high thermal conductivity of 4H-SiC ensures the convenient heat dissipation of 4H-SiC based high-power devices (Lidow et al., 2019; Higashiwaki et al., 2017). The unique features of 4H-SiC based high-power devices include high breakdown voltages, low power losses, and high switching speeds (Matsunami, 2004; Kimoto, 2015; Luo et al., 2019; Kimoto and Watanabe, 2020). Even though the defect control of 4H-SiC is mostly well-developed, the defects in 4H-SiC are found to significantly degrade the performance of 4H-SiC power devices. After decades of development, the device-killing micropipes and carrot defects have been successfully eliminated (Neudeck and Powell, 1994; Kimoto et al., 1999; Kimoto, 2014). While dislocations still act as dominant recombination centers, and are found to increase the leakage current and lower the breakdown voltage of 4H-SiC based high-power devices (Ewing et al., 2007; Friedrichs, 2008; Hamada et al., 2015; Łażewski et al., 2019).

According to the Burgers vectors and dislocation-line directions, dislocations in 4H-SiC can be classified as threading edge dislocations (TEDs), threading edge dislocations (TSDs), threading edge dislocations (TMDs), and basal plane dislocations (BPDs) (Nakamura et al., 2007; Li et al., 2022; Luo et al., 2022). It has been found that all the dislocations increase the leakage current of 4H-SiC power devices, and the effect of TSDs is more prominent than those of TEDs (Wahab et al., 2000; Berechman et al., 2010). As evidenced by synchrotron X-ray-topography (XRT) and transmission-electron-microscopy (TEM) investigations, TMDs dominate the configurations of the TSD/TMDs in 4H-SiC, while the effect of TMDs on the leakage current of 4H-SiC based high-power devices is still ambiguous (Onda et al., 2013; Konishi et al., 2019; Shinagawa et al., 2020). Meanwhile, the leakage current originating from BPDs was found in 4H-SiC *p*-*n* diodes and bipolar junction transistors (BJTs) (Muzykov et al., 2009; Skowronski and Ha, 2006; Ota et al., 2021). Because of the different Burgers vectors, different types of dislocations would generate different atomic disorders in 4H-SiC, and thus different degrees of the leakage current in 4H-SiC based high-power devices (Berechman et al., 2010; Nishio et al., 2022; Senzaki et al., 2006). However, the comparison of the type of dislocations on the leakage current of 4H-SiC is rarely understood. Furthermore, it is argued that the leakage current of threading dislocations, mainly TSDs and TEDs, is dominated by the surface pits formed by the outcrops of the threading dislocations, rather than the threading dislocations themselves (Fiorenza et al., 2020; Fujiwara et al., 2012a; Fujiwara et al., 2012b; Ohtani et al., 2012). However, Huang et al. found that the dislocation line of the TED in 4H-SiC Schottky barrier diodes (SBDs) controversially contributes to the leakage current (Huang et al., 2022). Therefore, identifying the degree of the leakage current induced by different types of dislocations, and discriminating the role of dislocations and dislocation-induced pits on the leakage current of 4H-SiC is critical to the optimization of 4H-SiC epilayers.

In this work, we investigate the effect of dislocations on the leakage current of homoepitaxial 4H-SiC by combining molten-KOH etching and the tunneling atomic force microscopy (TUNA) measurements. It turns out that the effect of dislocations on the reverse leakage current of 4H-SiC increases in the order to BPDs, TEDs, TSDs, and TMDs. The effect of dislocation line and the dislocation-related pit is also discriminated. We find that both the dislocation lines of TDs and the TD-related pits increase the reverse leakage current of 4H-SiC. The dislocation lines of TDs exert a more significant effect on the reverse leakage current of 4H-SiC, which gives rise to the nonuniform distribution of reverse leakage current throughout the TD-related pits. BPDs are also found to slightly increases the reverse leakage current, with the leakage current mainly concentrated at the core of the BPD. Compared to the effect of TDs, the effect of BPDs on the reverse leakage current of 4H-SiC is negligible.

2 Experimental methods

2.1 Epitaxy and molten-KOH etching of 4H-SiC thin film

The 30 μm 4H-SiC thin film was epitaxially grown by a hot-wall chemical vapor deposition (CVD) reactor on a 4° off-axis-sliced N-doped 4H-SiC (Skowronski and Kimoto, 2015). The homoepitaxy of 4H-SiC was carried out utilizing trichlorosilane ($SiHCl_3$) and ethylene (C_2H_4) as the growth sources of Si and C, respectively. The C/Si ratio was optimized to be 0.85, and hydrogen gas (H_2) was selected as the carrier gas. The flow rate of H_2 is 100 L/min. The growth temperature and pressure were 1,650°C and 100 mbar, respectively. Molten-KOH etching was performed at 550°C for 2 min in a Ni crucible to reveal the dislocation-related pits.

2.2 Characterizations

To discriminate the type of dislocations in 4H-SiC, the two-dimensional and three-dimensional morphologies of the dislocation-related pits were observed by the optical microscope (OM) (Olympus BX53M) and laser scanning confocal microscope (LSCM) (Zeiss LSM 900), respectively. The local leakage current of each type of dislocation was detected by the tunneling atomic force microscopy (TUNA) equipped with an atomic force microscope (AFM) (Dimension Icon, Bruker). TUNA is capable of imaging the local leakage current of semiconductors as low as 300 fA, with the conductive tip (PtIr-coated Si) acting as a nanoscale Schottky contact on the 4H-SiC epitaxial sample. TUNA measurements were performed by 256 × 256 points over 20 × 20 or 40 × 40 square micrometers. All images were taken at the scan speed of 0.3 Hz and a peak force of 3.5 μN.

3 Results and discussion

Figure 1A displays the OM image of the molten-KOH etched 4H-SiC epitaxial layer. The larger hexagonal pits, the smaller hexagonal pits, and the sea-shell pits correspond to the etch pits of TSDs/TMDs, TEDs, and BPDs, respectively (Konishi et al., 2019; Katsuno et al., 2011; Dong et al., 2013). By the statics of wafer-scale etch-pit density of different dislocations, the average dislocation densities of TSDs/TMDs, TEDs and BPDs are 3,770/cm^2, 2,352/cm^2, and 18/cm^2, respectively. To discriminate TMDs from TSDs, we take the three-dimensional morphologies of etch pits into account by LSCM. According to previous researches, the slope of etch pit of a TSD is unitarily steep and the etch pit ends by a deep point (Figures 1B, F). While the hexagonal pit of a TMD ends by a round plate, and the slope for the etch pit of a TMD is heterogeneous (Figures 1C, F).

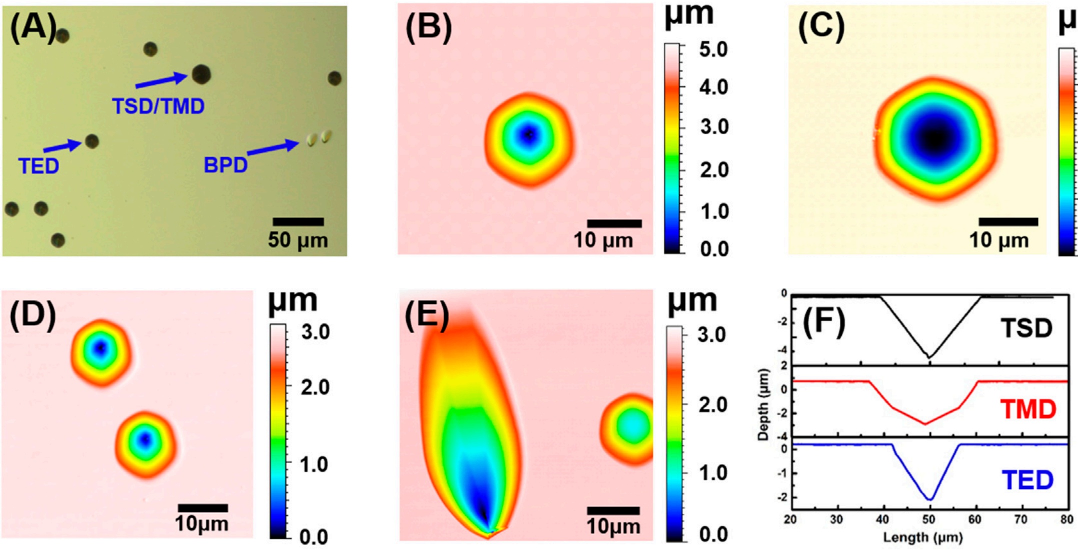

FIGURE 1
Representative OM images of etched 4H-SiC epitaxial layer samples **(A)**, the LSCM images of **(B)** TSD, **(C)** TMD, **(D)** TED, **(E)** BPD and depth profiles **(F)**.

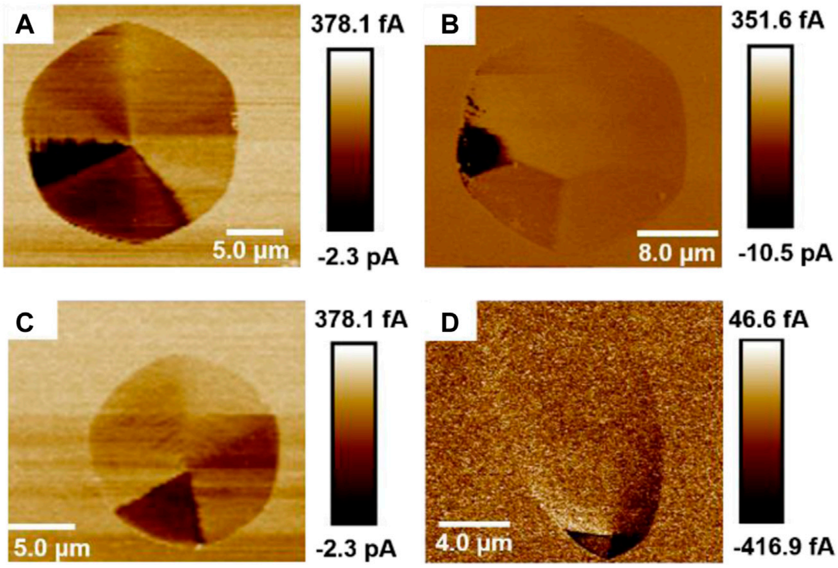

FIGURE 2
TUNA topography images of **(A)** TSD, **(B)** TMD, **(C)** TED, **(D)** BPD in 4H-SiC epitaxial layers.

After distinguishing all types of dislocations, we investigate the local leakage current of each type of dislocation by TUNA. As shown in Figures 2A–C, the leakage current throughout the pits of all types of TDs is higher than that in the dislocation-free region under the reverse bias. This indicates that TD-related pits exert a significant effect on the leakage current of 4H-SiC. Interestingly, we find that the magnitude of the leakage current depends on the lattice plane of the etch pit. Under the reverse bias of 6 V, the maximum leakage current of the TSD, TMD, and TED approaches 2.3 pA, 10.5 pA, and 1.5 pA, respectively. Furthermore, the BPD also gives rise to the leakage current through the BPD core. Compared to what happens in TDs, the BPD exerts a minor effect on the leakage current of 4H-SiC. Even when the reverse bias increases to 8 V, the BPD-induced leakage current is only 416.9 fA.

The inhomogeneity of leakage current throughout the dislocation pits of 4H-SiC can be understood as follows. It was found that the dislocation-relate pit composes six equivalent $(10\bar{1}1)$ planes in hexagonal GaN (Northrup et al., 1999). Given the similar crystal

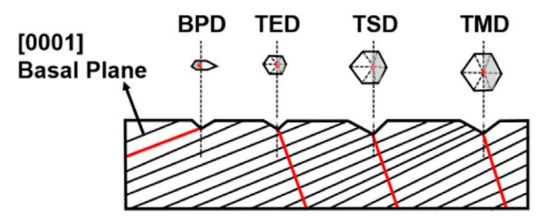

FIGURE 3
Schematic diagram showing the correlation between the dislocation lines and etch-pit morphologies in 4H-SiC epitaxial layers deposited on off-axis sliced substrates. The gray part of the etch pit denotes the etched surfaces near the dislocation lines.

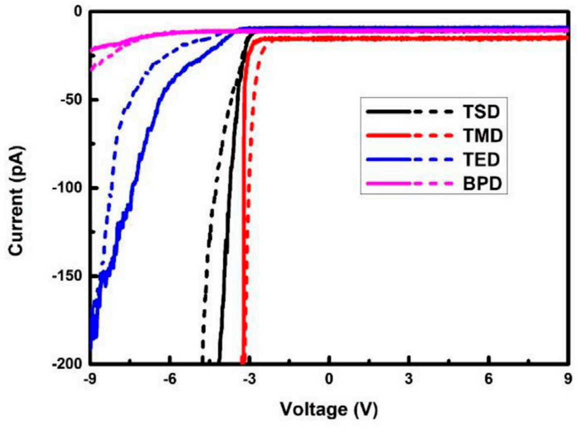

FIGURE 4
Localized *I-V* curves of TSD, TMD, TED, and BPD in 4H-SiC epitaxial layers.

symmetries and Burgers vectors of dislocations, the preferential etching along TDs also creates six equivalent $(10\bar{1}1)$ planes. Ideally, the leakage current would be uniformly distributed throughout the TD pits. However, due to the off-axis slicing of 4H-SiC substrates and the step-controlled homoepitaxy of 4H-SiC epitaxial layers, the [0001] crystallographic axis of the 4H-SiC epitaxial layer inclines towards the $[\bar{1}\bar{1}20]$ direction (Figure 3). This gives rise to the incline of the dislocation lines of TDs with respect to the surface. As shown in Figure 3, the gray part of the etch pit of TDs is closer to the dislocation lines of TDs than the white part. It is well established that the thermionic field emission theory dominates the reverse current of 4H-SiC-based Schottky diodes (Treu et al., 2001). The defect states of dislocation lines of TDs serve as transport paths of electrons and give rise to the increase of reverse leakage (Wang et al., 2021). Therefore, the reverse leakage current along the dislocation line of TDs would be the strongest. Since the gray part of TD-related pits locates closer to the dislocation lines of TDs, the enhanced reverse leakage current of the gray part of Figure 3 originates from the enhanced reverse leakage current dislocation lines of TDs. Therefore, the TUNA measurements verify that both the dislocation lines of TDs and TD-related pits participate in the reverse leakage current of 4H-SiC, of which the effect of dislocation lines of TDs is dominant.

At last, we compare the magnitude of reverse leakage current induced by different dislocations in 4H-SiC. It should be noted that the local *I-V* curves of the etch pits of different dislocations have been measured by 2-3 times at different etch pits, and the comparison of the leakage current is carried out at the same region of the etch pits. As shown in Figure 4, we find that the effect of dislocations on the reverse leakage current of 4H-SiC increases in the order of BPD, TED, TSD, and TMD. When the reverse bias voltage exceeds 2.55 V and 3.1 V, the leakage current along the TMD and TSD begin to sharply increases, respectively. TED exerts a minor effect on the reverse leakage current of 4H-SiC. When the reverse bias voltage is 3.55 V, the TED-induced leakage current gradually increases, with the degree of increase being gentler than what happens in TMD- and TSD-induced leakage current. The effect of TDs on the leakage current of 4H-SiC is associated with the Burgers vectors of TDs. The Burgers vectors of TMD, TSD, and TED are c + a, [000c], and $\frac{[11\bar{2}0]a}{3}$, respectively. The atomic distortions, and thus the strain field around dislocations increase in the order of BPD, TED, TSD, and TMD, which gives rise to the different extent of influences on the leakage current of 4H-SiC. Figure 4

4 Conclusion

In conclusion, we have clarified the effect of dislocations on the leakage current of homoepitaxial 4H-SiC by combining molten-KOH etching and TUNA measurements. It turns out that both the dislocation lines of TDs and the TD-related pits increase the reverse leakage current of 4H-SiC. The dislocation lines of TDs exert a more significant effect on the reverse leakage current of 4H-SiC, which gives rise to the nonuniform distribution of reverse leakage current throughout the TD-related pits. Due to the different Burgers vectors of TDs, the effect of TDs on the reverse leakage current of 4H-SiC increases in the order of TED, TSD, and TMD. BPDs are also found to slightly increases the reverse leakage current, with the leakage current mainly concentrated at the core of the BPD. Compared to the effect of TDs, the effect of BPDs on the reverse leakage current of 4H-SiC is negligible. Our work indicates that reducing the density of TDs, especially TMDs and TSDs, is key to improving the quality of 4H-SiC epitaxial layers and reducing the reverse leakage current of 4H-SiC based high-power devices.

Data availability statement

The raw data supporting the conclusion of this article will be made available by the authors, without undue reservation.

Author contributions

WG contributes to the design and implementation of the experiment, data analysis, and manuscript writing. GY contributes to the sample preparation and discussion of results. YQ contributes to the sample preparation and characterizations. XH contributes to the draft review and editing. CC contributes to the draft review and discussion of results. XP contributes to supervision, conceptualization, and the draft review. DY contributes to supervision, conceptualization, and draft review. RW contributes to the manuscript writing, discussion of results, supervision, and conceptualization.

Funding

This work was supported by Natural Science Foundation of China (Grant Nos. 62274143, U22A2075, 62204216), "Pioneer" and "Leading Goose" R&D Program of Zhejiang (Grant No. 2022C01021), National Key Research and Development Program of China (Grant No. 2018YFB2200101) and Zhejiang University Education Foundation Global Partnership Fund.

Conflict of interest

The authors declare that the research was conducted in the absence of any commercial or financial relationships that could be construed as a potential conflict of interest.

Publisher's note

References

Berechman, R. A., Skowronski, M., Soloviev, S., and Sandvik, P. (2010). Electrical characterization of 4H–SiC avalanche photodiodes containing threading edge and screw dislocations. *J. Appl. Phys* 107, 114504. doi:10.1063/1.3432663

Cooper, J. A., and Agarwal, A. (2002). SiC power-switching devices-the second electronics revolution. *Proc. IEEE Inst. Electr. Electron Eng* 90, 956–968. doi:10.1109/JPROC.2002.1021561

Dong, L., Zheng, L., Liu, X. F., Zhang, F., Yan, G. G., and Li, X. G., (2013). Defect revelation and evaluation of 4H silicon carbide by optimized molten KOH etching method. *Mat. Sci. Forum* 740, 243–246. doi:10.4028/www.scientific.net/msf.740-742.243

Ewing, D. J., Porter, L. M., Wahab, Q., Ma, X., Sudharshan, T. S., and Tumakha, S., (2007). Inhomogeneities in Ni∕4H-SiC Schottky barriers: Localized Fermi-level pinning by defect states. *J. Appl. Phy* 101, 114514. doi:10.1063/1.2745436

Fiorenza, P., Alessandrino, M. S., Carbone, B., Martino, C. D., Russo, A., and Saggio, M., (2020). Understanding the role of threading dislocations on 4H-SiC MOSFET breakdown under high temperature reverse bias stress. *Nanotechnology* 31, 125203. doi:10.1088/1361-6528/ab5ff6

Friedrichs, P. (2008). Silicon carbide power-device products–Status and upcoming challenges with a special attention to traditional, nonmilitary industrial applications. *Phys. status solidi B* 245, 1232–1238. doi:10.1002/pssb.200743478

Fujiwara, H., Naruoka, H., Konishi, M., Hamada, K., Katsuno, T., and Ishikawa, T., (2012). Impact of surface morphology above threading dislocations on leakage current in 4H-SiC diodes. *Appl. Phys. Lett* 101, 042104. doi:10.1063/1.4738886

Fujiwara, H., Naruoka, H., Konishi, M., Hamada, K., Katsuno, T., and Ishikawa, T., (2012). Relationship between threading dislocation and leakage current in 4H-SiC diodes. *Appl. Phys. Lett* 100, 242102. doi:10.1063/1.4718527

Hamada, K., Hino, S., Miura, N., Watanabe, H., Nakata, S., and Suekawa, E., (2015). 3.3 kV/1500 A power modules for the world's first all-SiC traction inverter. *Jpn. J. Appl. Phys* 54, 04DP07. doi:10.7567/JJAP.54.04DP07

Higashiwaki, M., Kuramata, A., Murakami, H., and Kumagai, Y. (2017). State-of-the-art technologies of gallium oxide power devices. *J. Phys. D. Appl. Phys* 50, 333002. doi:10.1088/1361-6463/aa7aff

Huang, J. R., Chen, T. W., Lee, J. W., Huang, C. F., and Hong, L. S. (2022). A perspective on leakage current induced by threading dislocations in 4H-SiC Schottky barrier diodes. *Mat. Lett* 310, 131506. doi:10.1016/j.matlet.2021.131506

Katsuno, T., Watanabe, Y., Hirokazu, F., Konishi, M., Yamamoto, T., and Endo, T. (2011). New separation method of threading dislocations in 4H-SiC epitaxial layer by molten KOH etching. *Mat. Sci. Forum* 679, 298–301. doi:10.4028/www.scientific.net/msf.679-680.298

Kimoto, T., and Cooper, J. A. (2014). *Fundamentals of silicon carbide technology: Growth, characterization, devices and applications*. Singapore: Wiley.

Kimoto, T. (2015). Material science and device physics in SiC technology for high-voltage power devices. *J. Appl. Phys* 54, 040103. doi:10.7567/JJAP.54.040103

Kimoto, T., Miyamoto, N., and Matsunami, H. (1999). Performance limiting surface defects in SiC epitaxial pn junction diodes. *IEEE Trans. Electron Devices* 46, 471–477. doi:10.1109/16.748864

Kimoto, T., and Watanabe, H. (2020). Defect engineering in SiC technology for high-voltage power devices. *Appl. Phys. Express* 13, 120101. doi:10.35848/1882-0786/abc787

Konishi, K., Nakamura, Y., Nagae, A., Kawabata, N., Tanaka, T., and Tomita, N., (2019). Direct observation and three-dimensional structural analysis for threading mixed dislocation inducing current leakage in 4H–SiC IGBT. *Jpn. J. Appl. Phys* 59, 011001. doi:10.7567/1347-4065/ab5ee8

Łażewski, J., Jochym, P. T., Piekarz, P., Sternik, M., Parlinski, K., and Cholewin´ski, J., (2019). DFT modelling of the edge dislocation in 4H-SiC. *J. Mat. Sci* 54, 10737–10745. doi:10.1007/s10853-019-03630-5

Li, J., Luo, H., Yang, G., Zhang, Y., Pi, X. D., and Yang, D. R., (2022). Nitrogen decoration of basal-plane dislocations in 4H-SiC. *Phys. Rev. Appl* 17, 054011. doi:10.1103/PhysRevApplied.17.054011

Lidow, A., De Rooij, M., Strydom, J., Strydom, J., and Glaser, J. (2019). *GaN transistors for efficient power conversion*. John Wiley & Sons. New Jersey, USA.

Luo, H., Li, J., Yang, G., Zhu, R., Zhang, Y., and Wang, R., (2022). Electronic and optical properties of threading dislocations in n-type 4H-SiC. *ACS Appl. Electron. Mat* 4, 1678–1683. doi:10.1021/acsaelm.1c01330

Luo, X., Liao, T., Wei, J., Fang, J., Yang, F., and Zhang, B. (2019). A novel 4H-SiC trench MOSFET with double shielding structures and ultralow gate-drain charge. *J. Semicond* 40, 052803. doi:10.1088/1674-4926/40/5/052803

Matsunami, H. (2004). Technological breakthroughs in growth control of silicon carbide for high power electronic devices. *J. Appl. Phys* 43, 6835–6847. doi:10.1143/JJAP.43.6835

Muzykov, P. G., Kennedy, R. M., Zhang, Q. J., Capell, C., Burk, A., and Agarwal, A., (2009). Physical phenomena affecting performance and reliability of 4H–SiC bipolar junction transistors. *Microelectron. Reliab* 49, 32–37. doi:10.1016/j.microrel.2008.10.009

Nakamura, D., Yamaguchi, S., Gunjishima, I., Hirosea, Y., and Kimotob, T. (2007). Topographic study of dislocation structure in hexagonal SiC single crystals with low dislocation density. *J. Cryst. Growth* 304, 57–63. doi:10.1016/j.jcrysgro.2007.02.002

Neudeck, P. G., and Powell, J. A. (1994). Performance limiting micropipe defects in silicon carbide wafers. *IEEE Electron Device Lett* 15, 63–65. doi:10.1109/55.285372

Nishio, J., Ota, C., and Iijima, R. (2022). Structural study of single Shockley stacking faults terminated near substrate/epilayer interface in 4H-SiC. *Jpn. J. Appl. Phys* 61, SC1005. doi:10.35848/1347-4065/ac3a91

Northrup, J. E., Romano, L. T., and Neugebauer, J. (1999). Surface energetics, pit formation, and chemical ordering in InGaN alloys. *Appl. Phys. Lett* 74, 2319–2321. doi:10.1063/1.123837

Ohtani, N., Ushio, S., Kaneko, T., Aigo, T., Katsuno, M., and Fujimoto, T., (2012). Tunneling atomic force microscopy studies on surface growth pits due to dislocations in 4H-SiC epitaxial layers. *J. Electron. Mat* 41, 2193–2196. doi:10.1007/s11664-012-2133-3

Onda, S., Watanabe, H., Kito, Y., Kondo, H., Uehigashi, H., and Hosokawa, N., (2013). Transmission electron microscope study of a threading dislocation with and its effect on leakage in a 4H–SiC MOSFET. *Philos. Mag. Lett* 93, 439–447. doi:10.1080/09500839.2013.798047

Ota, C., Nishio, J., Okada, A., and Lijima, R. (2021). Origin and generation process of a triangular single shockley stacking fault expanding from the surface side in 4H-SiC PIN diodes. *J. Electron. Mat* 50, 6504–6511. doi:10.1007/s11664-021-09186-y

Senzaki, J., Kojima, K., Kato, T., Shimozato, A., and Fukuda, K. (2006). Correlation between reliability of thermal oxides and dislocations in n-type 4H-SiC epitaxial wafers. *Appl. Phys. Lett* 89, 022909. doi:10.1063/1.2221525

Shinagawa, N., Izawa, T., Manabe, M., Yamochi, T., and Ohtani, N. (2020). Populations and propagation behaviors of pure and mixed threading screw dislocations in physical vapor transport grown 4H-SiC crystals investigated using X-ray topography. *Jpn. J. Appl. Phys* 59, 091002. doi:10.35848/1347-4065/abab46

Skowronski, M., and Ha, S. (2006). Degradation of hexagonal silicon-carbide-based bipolar devices. *J. Appl. Phys* 99, 011101. doi:10.1063/1.2159578

Skowronski, M., and Kimoto, T. (2015). *Handbook of crystal growth*. Silicon carbide epitaxy[M], North-Holland, 1135–1167.

Treu, M., Rupp, R., Kapels, H., and Bartsch, W. (2001). Temperature dependence of forward and reverse characteristics of Ti, W, Ta and Ni Schottky diodes on 4H-SiC. *Mat. Sci. Forum* 353, 679–682. doi:10.4028/www.scientific.net/msf.353-356.679

Wahab, Q., Ellison, A., Henry, A., Janzen, E., Hallin, C., and Di Persio, J., (2000). Influence of epitaxial growth and substrate-induced defects on the breakdown of 4H–SiC Schottky diodes. *Appl. Phys. Lett* 76, 2725–2727. doi:10.1063/1.126456

Wang, J. F., Yan, F. F., Li, Q., Liu, Z., Liu, H., and Guo, G., (2020). Coherent control of nitrogen-vacancy center spins in silicon carbide at room temperature. *Phys. Rev. Lett* 124, 223601. https://doi. org/doi:10.1103/PhysRevLett.124.223601

Wang, R., Xu, J., Zhang, S., Zhang, Y., Zheng, P., and Cheng, Z., (2021). Reducing the reverse leakage current of AlGaN/GaN heterostructures via low-fluence neutron irradiation. *J. Mat. Chem. C* 9, 3177–3182. doi:10.1039/d0tc05652a